Beth Israel Deaconess Medical Center
A member of CareGroup

Harvard Medical School

The Importance of Medical Imaging

Charles R.G. Guttmann, M.D.
Robert E. Lenkinski, PhD

Image: Philips

PET

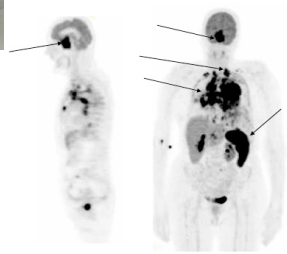

CT

Image: Toshiba

Image: GE

MRI

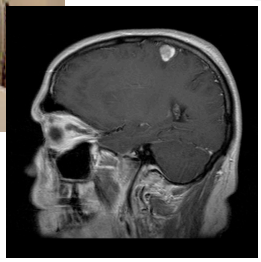

Ultrasound

Image: Siemens

The Evolution of Clinical Imaging

- Technical advances-improving the technical quality of the images
- Improving the ability to review and interpret the images-digital age

Trends

- Structure-function (anatomy-physiology/metabolism)
- Diagnostic accuracy (sensitivity-specificity)

The Continued Evolution of Clinical Imaging

- Extracting the maximum amount of diagnostic information from the images
- Relating imaging features to pathology, physiology, and biology

Contrast Enhanced MRI of the Breast Has Diagnostic Value

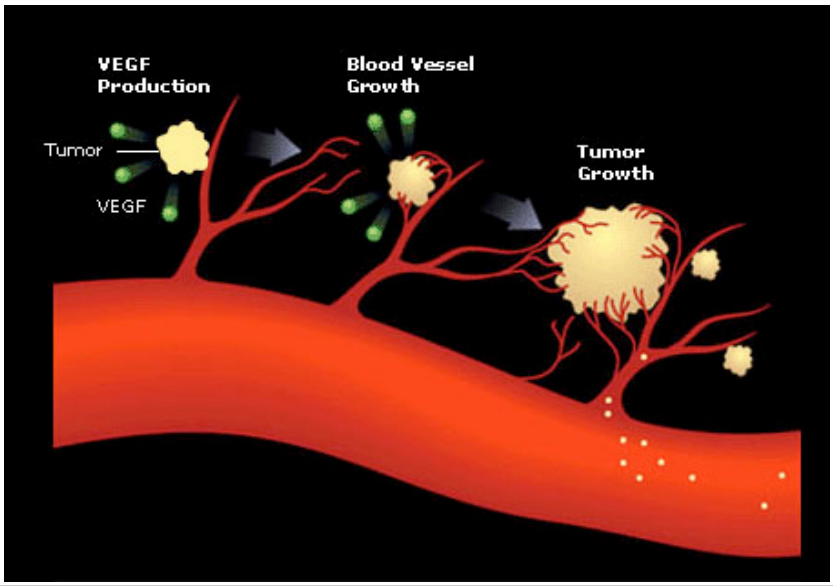

Behavior of Contrast Agent in Body

- **Depends on:**
  - **Cellular density or "Extracellular Volume Fraction"**
  - **Blood vessel permeability "Microvascular Permeability"**

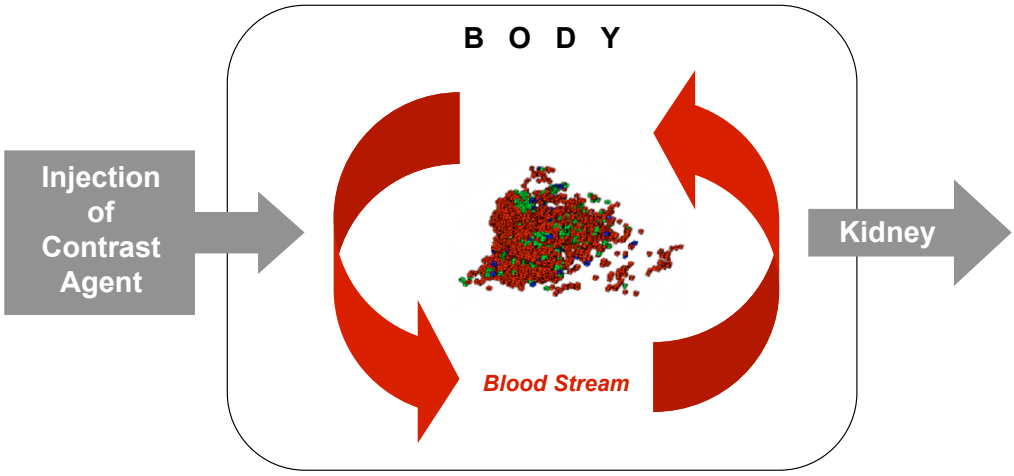

Dynamic Contrast Enhanced MRI (DCEMRI)

Components

- "High-field" MRI machine (1.0 tesla or greater)
- Standard breast coil
- Gadolinium contrast agent (GdDTPA)
- Images taken at several time points (spatial vs temporal resolution
- Software algorithm processes data for either parametric maps or semi-quantitative plots

Christiane Katharina Kuhl, MD
Peter Mielcareck, MD
Sven Klaschik, MD
Claudia Leutner, MD
Eva Wardelmann, MD
Jürgen Gieseke, PhD
Hans H. Schild, MD

Dynamic Breast MR Imaging: Are Signal Intensity Time Course Data Useful for Differential Diagnosis of Enhancing Lesions?[1]

Radiology 1999; 211:101–110

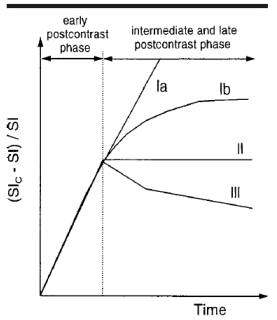

Figure 1. Schematic drawing of the time–signal intensity curve types. Type I corresponds to a straight (*Ia*) or curved (*Ib*) line; enhancement continues over the entire dynamic study. Type II is a plateau curve with a sharp bend after the initial upstroke. Type III is a washout time course ($[SI_c - SI]/SI$).

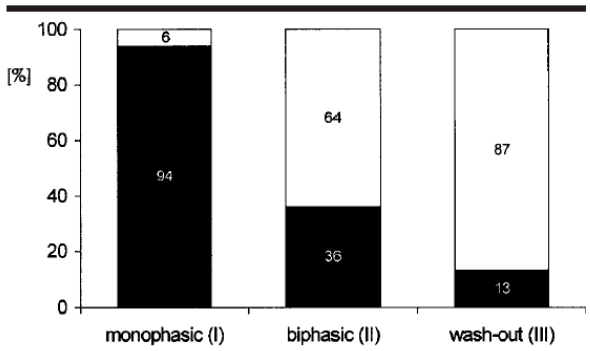

Figure 4. Bar graph shows the prevalence of benign (black bars) and malignant (white bars) lesions for the three different signal intensity time courses.

Color Coding by the 3TP Algorithm

Time Points
t_0 = 0 minutes
t_1 = 2 minutes

Wash-in rate
color intensity
(256 shades)

Wash-out pattern
determines color
(3 shades)

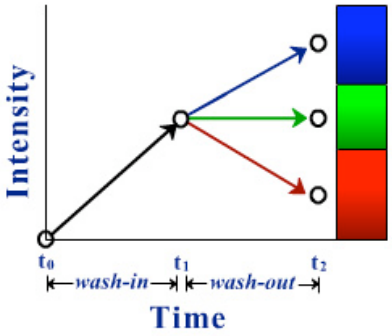

Breast Cases: Cancer

MRI Images – Same Slice

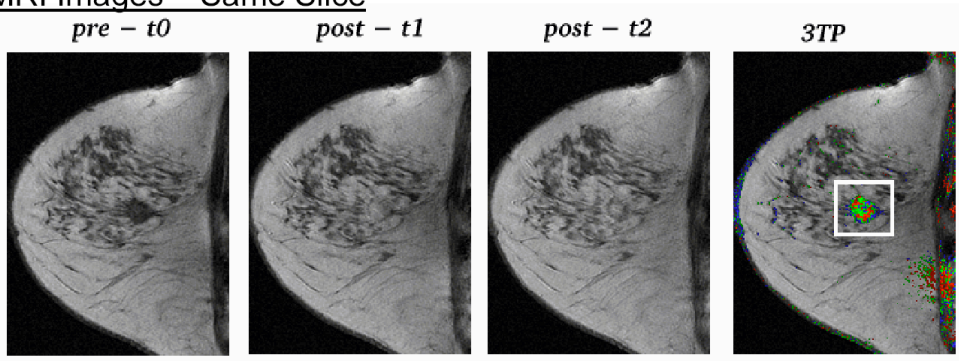

Additional Slices

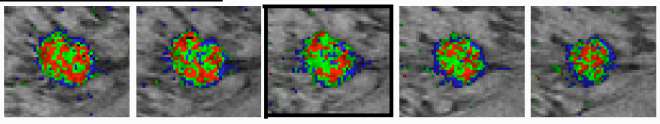

Breast Cases: Fibroadenoma

MRI Images – Same Slice

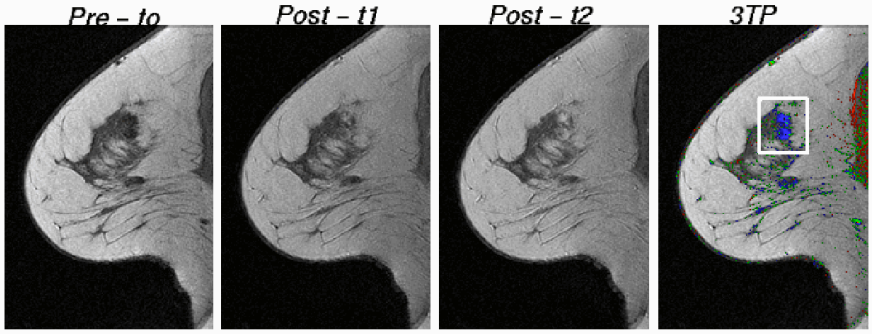

Individual Slices

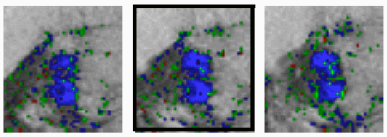

VEGF Mediated Angiogenesis

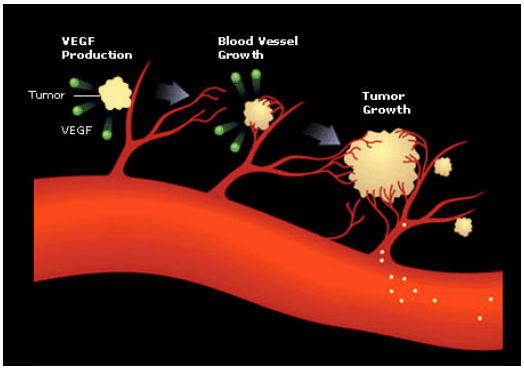

Anti-Angiogenesis

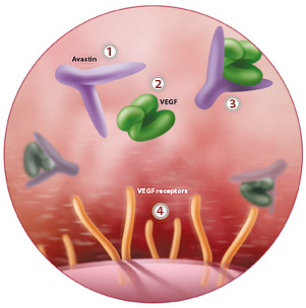

Imaging angiogenesis-MR-DSC, DCE, ASL

Brain Tumors-GBM's

Paradoxical improvement in imaging parameters followed by clinical progression or worsening of Imaging parameters with no tumor progression

Beyond "Radiologic-Pathologic Correlation"[1]

King C. P. Li, MD, MBA

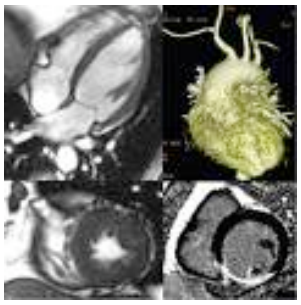

Scale

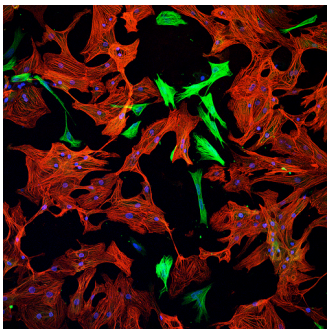

Cardiomyocytes (red) and fibroblasts (green) isolated from chicken embryo heart.

Radiogenomics in Diagnosis

nature biotechnology

Decoding global gene expression programs in liver cancer by noninvasive imaging

Eran Segal[1], Claude B Sirlin[2], Clara Ooi[4], Adam S Adler[5], Jeremy Gollub[6], Xin Chen[8], Bryan K Chan[2], George R Matcuk[7], Christopher T Barry[3], Howard Y Chang[5] & Michael D Kuo[2]

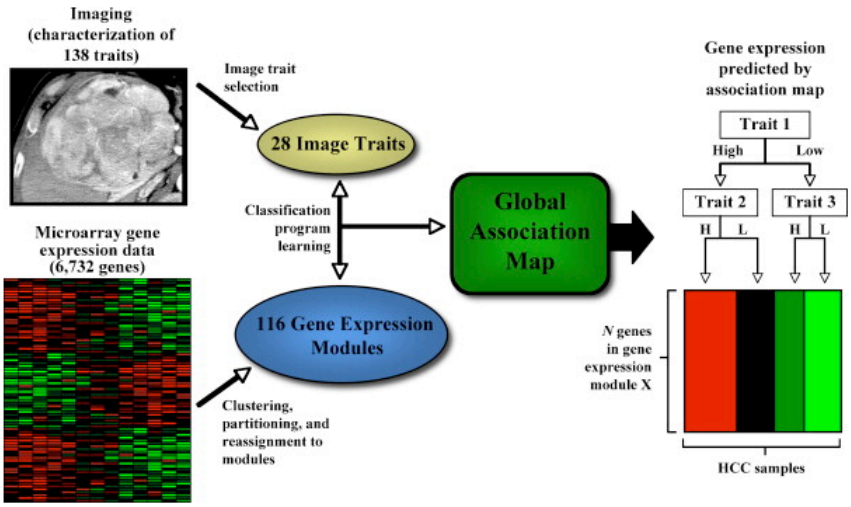

Fig. 2. Knowledge of imaging traits allows approximate reconstruction of a given HCC sample's gene expression pattern, as reported by Segal et al. [8]. The authors created a global "association map" between imaging features and gene expression. Expression variation of 6732 genes, as measured by microarray data and captured by 116 gene expression "modules", was sufficiently reconstructed by a combination of only 28 imaging traits. The decision tree of imaging trait expression patterns is used to predict variation of expression in a given gene expression module. Each split in the tree is determined by variation of an imaging trait, while each terminus identifies a group of samples that share a similar expression pattern of genes in a particular gene expression module.

Otto Warburg, 1931

Cancer cells will undergo glycolysis even in the presence of oxygen

Opposite of the Pasteur effect

Otto Heinrich Warburg

Otto Heinrich Warburg

Born	October 8, 1883 Freiburg, Baden, Germany
Died	August 1, 1970 (aged 86) Berlin, West Germany
Nationality	German
Fields	Cell biology
Institutions	Kaiser Wilhelm Institute for Biology
Alma mater	University of Berlin University of Heidelberg
Doctoral advisor	Emil Fischer Ludolf von Krehl
Known for	Pathogenesis of cancer
Notable awards	Nobel Prize in Physiology or Medicine (1931)

Figure 1. Molecular underpinnings of the Warburg effect

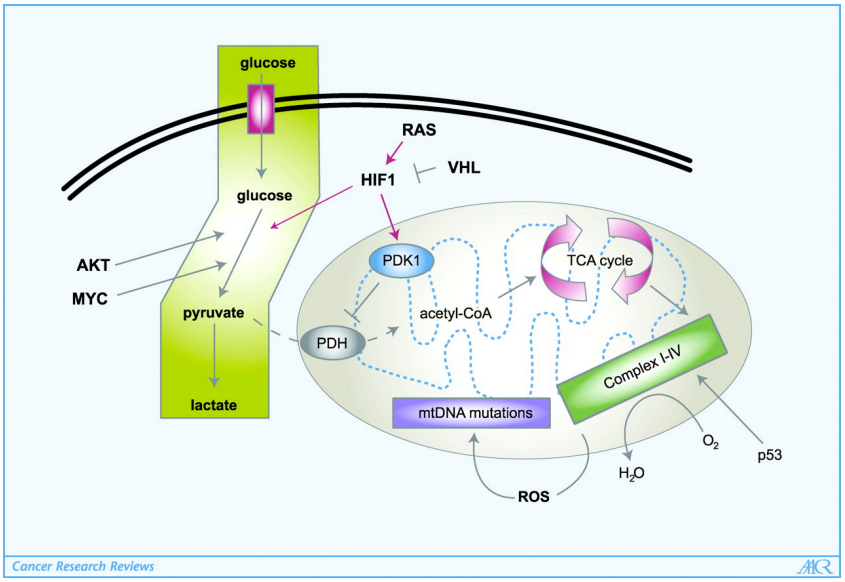

Kim, J.-w. et al. Cancer Res 2006;66:8927-8930

Good News

We can image glycolysis with FDG PET

Glucose and FDG metabolism.

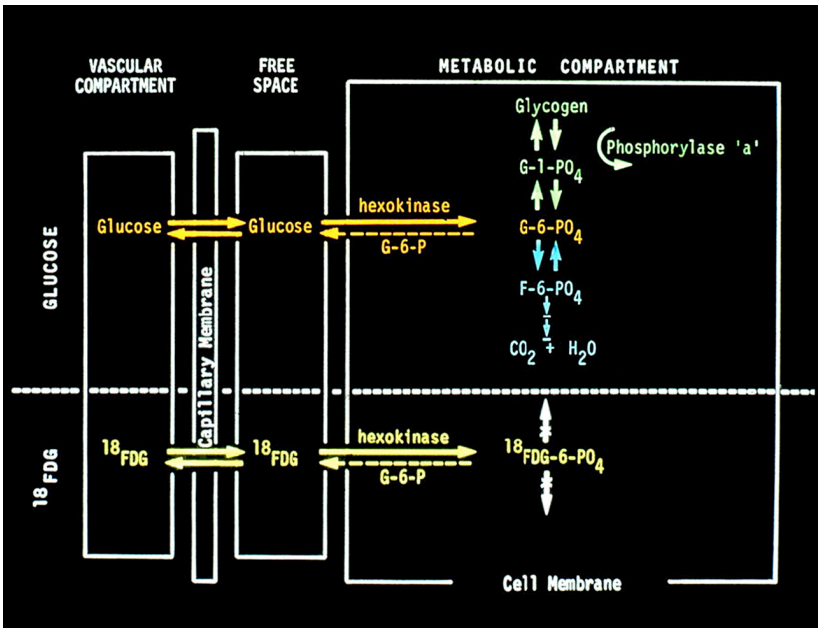

Hoffman J M , Gambhir S S Radiology 2007;244:39-47

Radiology

Glucose and FDG metabolism.

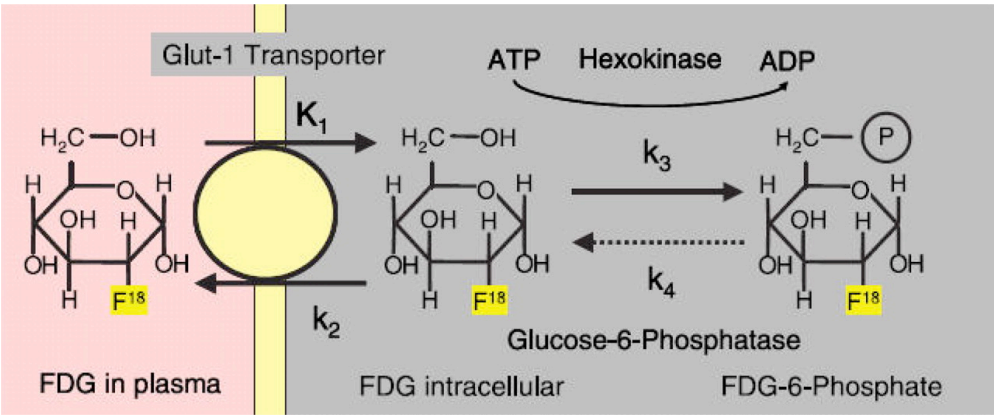

Hoffman J M , Gambhir S S Radiology 2007;244:39-47

Radiology

Glycolyisis is common trait of metastatic cancers

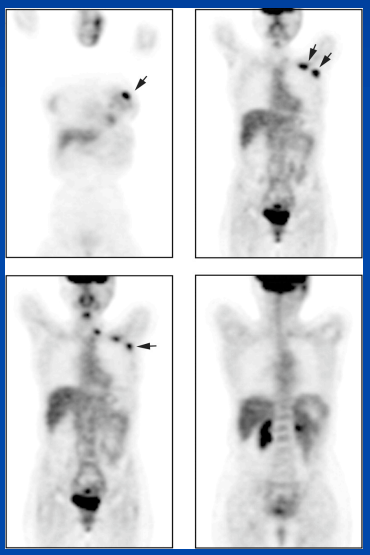

ELSEVIER
SCIENCE DIRECT
Genomics 84 (2004) 1014–1020
GENOMICS
www.elsevier.com/locate/ygeno

Genes of glycolysis are ubiquitously overexpressed in 24 cancer classes

B. Altenberg[a,*], K.O. Greulich[b]

[a]Bioinformatics Group, European Molecular Biology Laboratory, Meyerhofstrasse 1, D-69117 Heidelberg, Germany
[b]Department of Single Cell and Single Molecule Techniques, Institute for Molecular Biotechnology, Beutenbergstrasse 11, D-07745 Jena, Germany

Received 27 July 2004; accepted 8 August 2004
Available online 25 September 2004

Table 4. Sensitivity and Specificity of FDG PET for detection of metastases (data culled from reference *(39)*)

Cancer metastasis	Sens		Spec	
	Range	median	range	median
NSCLC - mediastinal	67-100	94	84-100	100
CRC - LN & hepatic	73-100	95	96-100	100
Melanoma	70-100	100	77-100	100
Lymphoma	50-100	80	87-100	92
Breast	83-100	97	75-100	97
Cervical – LN	3-100	72	92-100	100
Esophageal – distant	69-100	91	67-93	91
Prostate – LN & bone	40-75	65	n/a	

J. Nuc. Med. 49(2):24S-42S, 2008

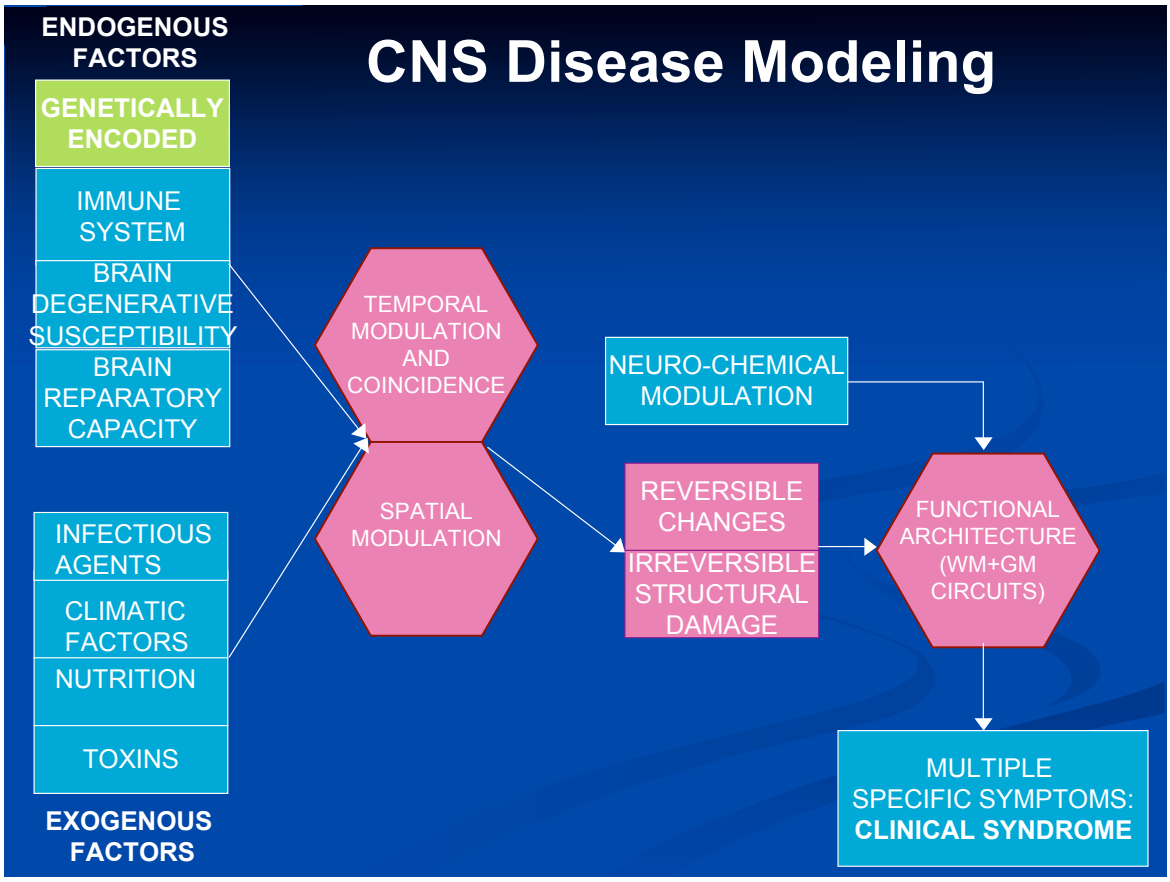

Time Series Analysis: Can "Chronobiopsy" of individual lesions predict pathological stage and disease progression?

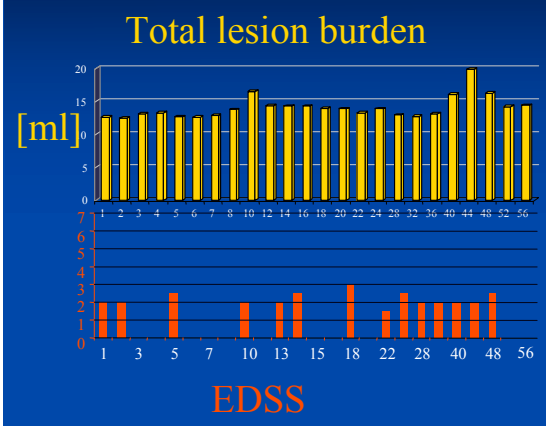

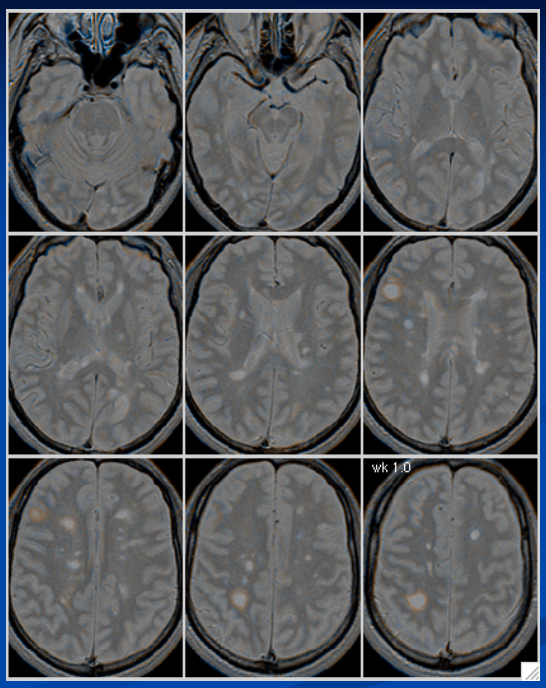

Timing and Sequence of Pathological Processes

Inflammation

~ days - weeks

- Blood Brain Barrier breakdown
- Edema
- Cellular Infiltration

Degeneration

- Demyelination
- Axonal/Neuronal Damage

~ weeks-months

Repair

~ months-years?

- Macrophage activity
- Astrocytosis
- Remyelination
- Axonal Repair?

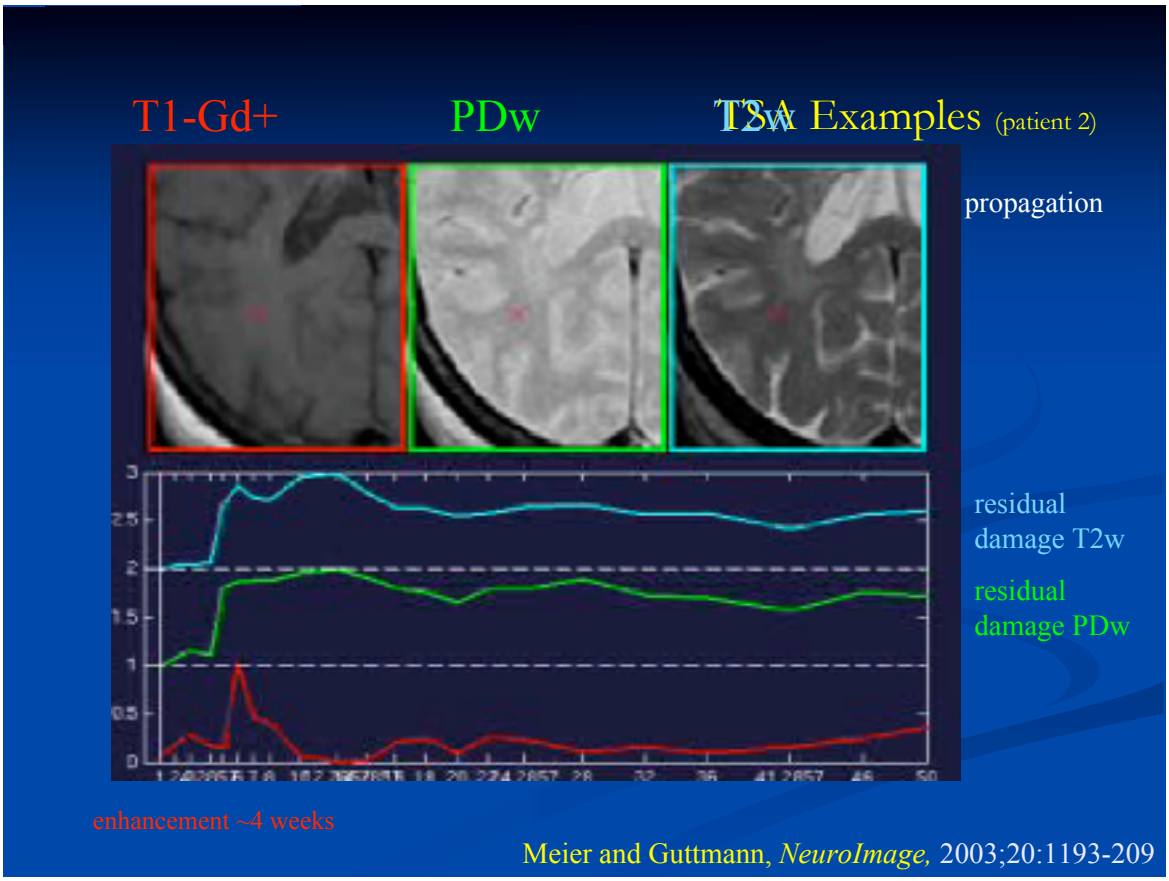
T1-Gd+
PDw
T2w
Examples (patient 2)
propagation
residual damage T2w
residual damage PDw
enhancement ~4 weeks
Meier and Guttmann, NeuroImage, 2003;20:1193-209

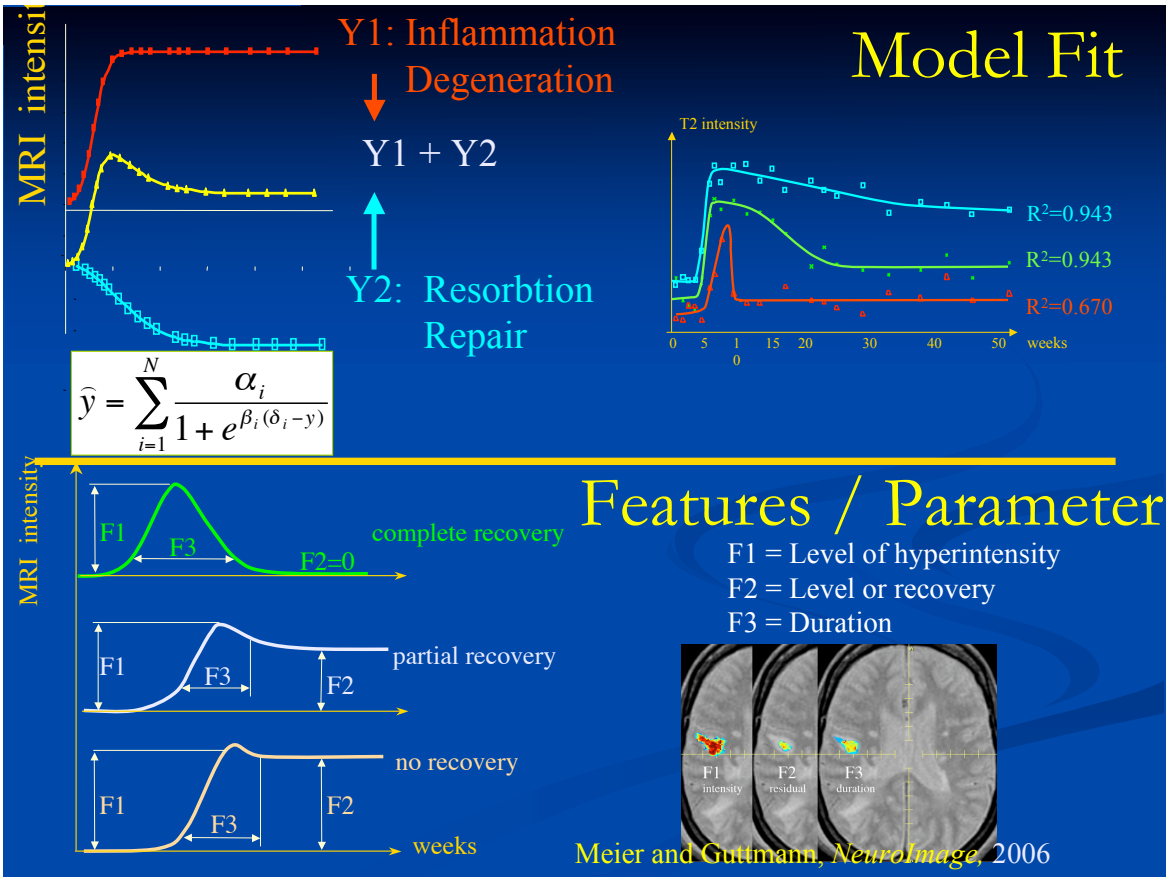
MRI intensi
Y1: Inflammation
Degeneration
Y1 + Y2
Y2: Resorbtion
Repair
Model Fit
T2 intensity
R²=0.943
R²=0.943
R²=0.670
weeks
$\hat{y} = \sum_{i=1}^{N} \frac{\alpha_i}{1 + e^{\beta_i(\delta_i - y)}}$
MRI intensity
F1
F3
F2=0
complete recovery
partial recovery
F2
no recovery
weeks
Features / Parameter
F1 = Level of hyperintensity
F2 = Level or recovery
F3 = Duration
F1 intensity
F2 residual
F3 duration
Meier and Guttmann, NeuroImage, 2006

- reduced short-term lesion recovery was associated with greater atrophy rates and disability.
- smaller lesions disproportionally more damaging: leaving more residual, associated with greater disability.

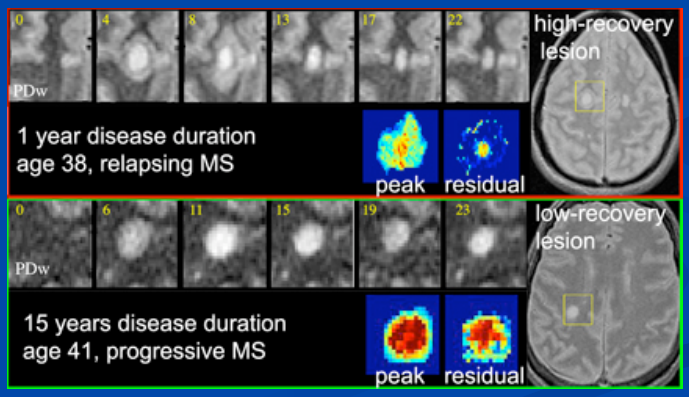

Meier,Weiner, Guttmann, *AJNR,* 2007, 28:1956-63

Spatial Analysis: Does normal cerebral perfusion predict lesion prevalence at different locations?

Fact: Repair Does Occur in MS

1. When?

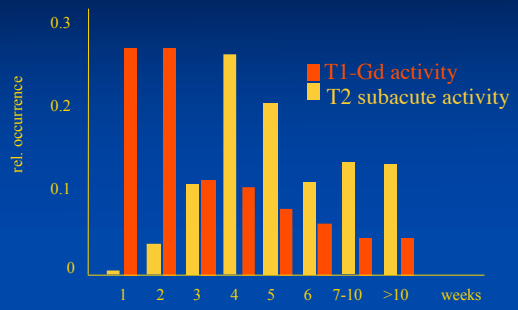

2. Under what Conditions?

Does perfusion modulate brain repair?

Voxel Based Morphometry (VBM)

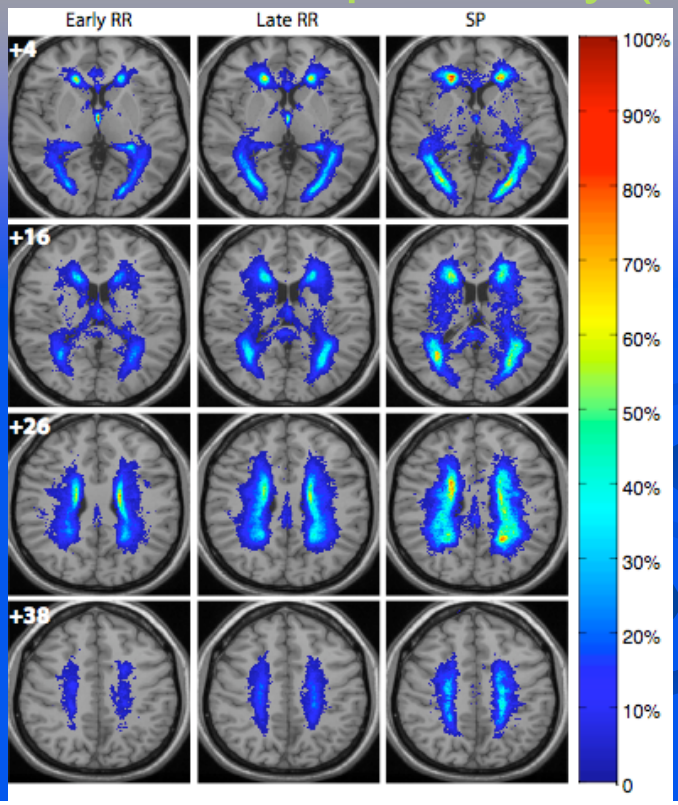

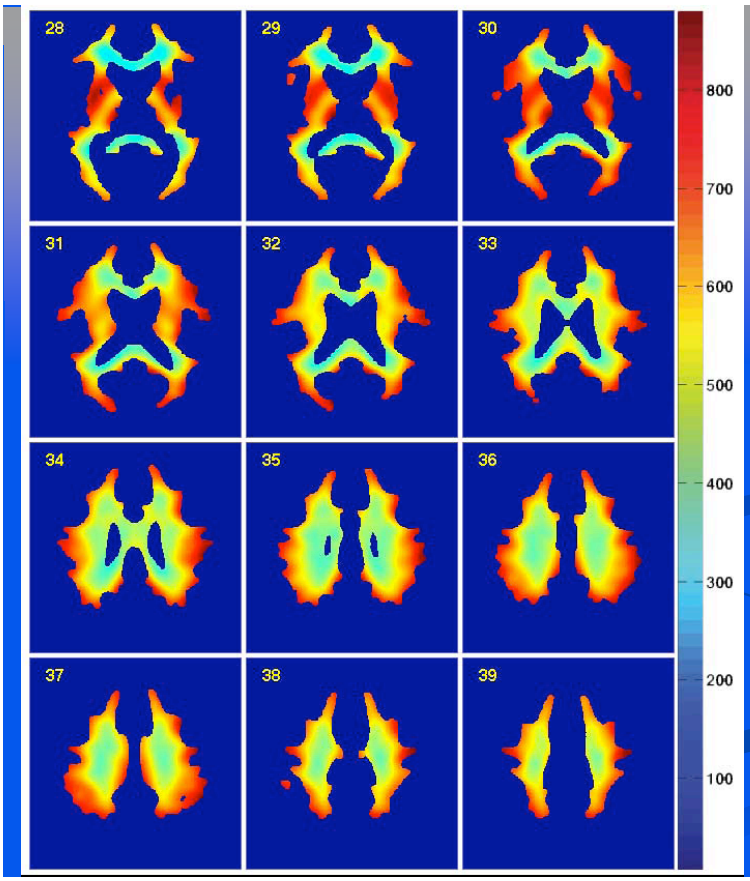

Based Morphometry (CBM)

Healthy Perfusion Atlas

Tc-99m SPECT N = 47

Context Based Morphometry (CBM) Early MS (N=89)

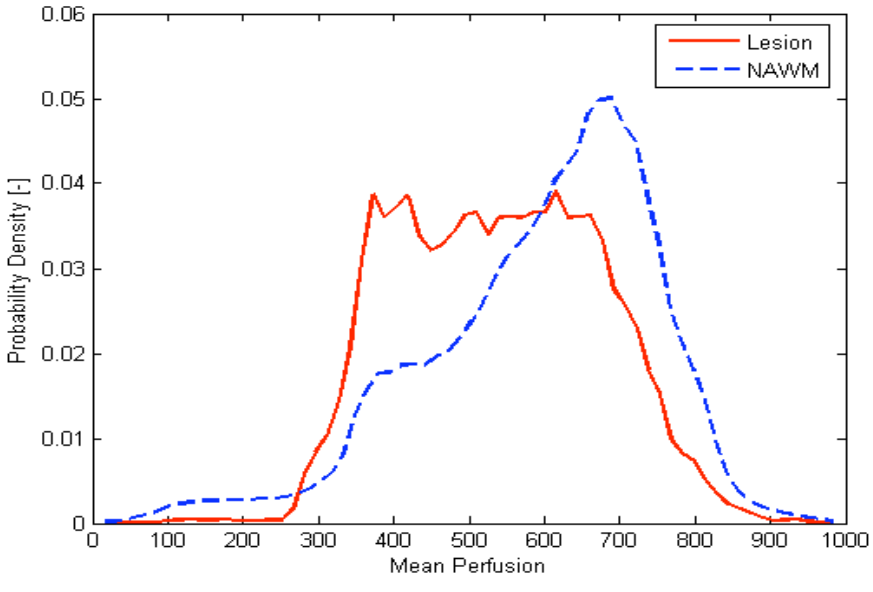

Context Based Morphometry (CBM) MS (N=1249)